

INFLUENCE OF CARBON FIBER REINFORCED POLYMERS ON UPGRADING SHEAR BEHAVIOR OF RC COUPLING BEAMS*

A. KHEYRODDIN^{1,**}, H. NADERPOUR¹, G. GHODRATI AMIRI² AND S.R. HOSEINI VAEZ¹

¹Dept. of Civil Engineering, Semnan University, Semnan, I. R. of Iran
Email: akheirodin@semnan.ac.ir

²School of Civil Engineering, Iran University of Science and Technology, Tehran, I. R. of Iran

Abstract– Shear wall with coupling beam is a very effective means of providing lateral bracing for buildings subjected to earthquakes. The strength, stiffness and ductility of coupling beams considerably influence the behavior of coupled wall systems, since even the local failure of each coupling beam could lead to the global failure of the structure. In this paper, two common efficient strengthening methods for improving the behavior of RC coupling beams have been investigated. The nominal shear strength of an FRP-strengthened concrete member can be determined by adding the contribution of the FRP external shear reinforcement to the contributions from the reinforcing steel and the concrete. Numerical studies were conducted to analyze three groups of RC coupling beams, of which one was strengthened by externally bonded steel plates and the other two strengthened with FRP sheets. Fiber Reinforced Polymer (FRP) composites have found increasingly wide applications in structural engineering due to their high strength to weight ratio, high corrosion resistance and ease of installation. The FRP-strengthened groups differ on how the FRP is attached to the coupling beam. The material properties used for modeling the concrete, reinforcement and FRP were adopted due to experimental data. Based on the numerical results, strengthening using steel plates upgraded the lateral load bearing capacity up to 66%, while the improvement in deformation capacity was about 50%. Also, the FRP sheets could considerably enhance the strength and deformation capacity of coupling beams; as in the most effective procedure (wrapping) increased the shear force by 84% and chord rotation capacity by 77%.

Keywords– Coupling beam, FRP, seismic, strength, wrapping, externally bonded

1. INTRODUCTION

The term "composite wall system" refers to a number of possible configurations including: (1) cantilever composite walls, where steel or FRP components are embedded in or attached to RC walls, (2) Hybrid dual systems, where RC walls are placed in parallel with steel moment frames and (3) Hybrid coupled walls, where composite beams (with steel or FRP sheets) are used to couple two or more RC or composite walls in series [1]. The behavior of the third group has been investigated in this study.

Shear walls with coupling beams are a very effective means of providing lateral bracing for buildings subjected to earthquakes. In a coupled shear wall more openings are allowed, providing more functional flexibility, which is so important in architecture. Furthermore, by coupling individual flexural shear walls, the lateral-load resisting behavior changes to one where overturning moments are resisted partially by an axial compression–tension couple across the wall system rather than by flexural action of the individual walls (Fig. 1) [2]. Hence, dissipation of the input energy can be distributed over the height of the building in the coupling beams rather than concentrating on the bottom of the wall piers, where structural damage could be severe.

*Received by the editors July 25, 2009; Accepted February 8, 2011.

**Corresponding author

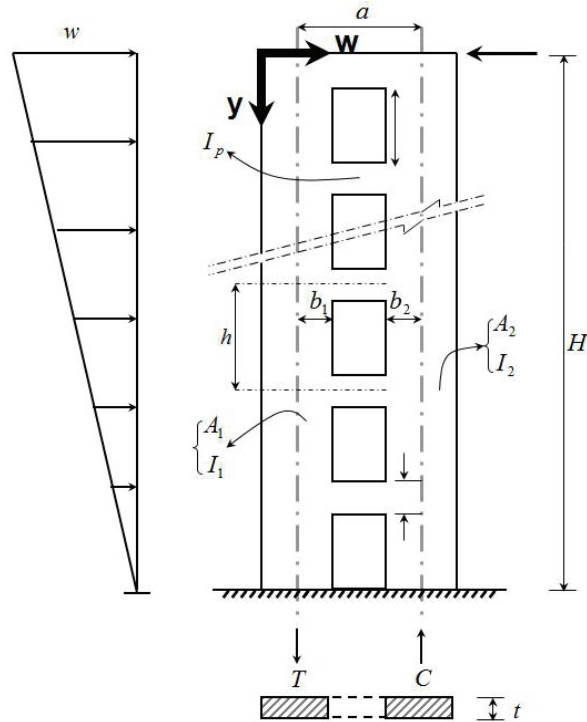


Fig. 1. Lateral load resisting mechanism of coupled shear wall [2]

There has been a considerable body of work investigating the response of coupled wall structures. The emphasis of the majority of studies has been concentrated on optimizing the overall response of the walls and design process [3].

Some researchers investigated the seismic behavior of steel coupling beams as an alternative for ordinary RC ones and have shown that the lateral stiffness and strength of concrete shear walls can be increased by coupling the shear walls using embedded steel beams [4, 5]. Although this method has been shown to be effective, it is not applicable where strengthening or rehabilitating is required.

There are two methods for strengthening or retrofitting the shear behavior of existing RC beams. The first method is attaching steel plates to the external surfaces of beams by means of bolting or bonding which has been investigated by several researchers. Barnes et al. (2001) studied the effects of externally attaching the steel plates to the surfaces of RC beams on shear behavior by means of bonding and bolting [6]. Strengthening the shear capacity of RC beams by bolted steel plates on the external surfaces has been investigated by Subedi and Baglin (1998) and the results indicated the enhancement of shear and flexural strengths of the beams [7].

The second and more recent method of retrofitting the RC beams is using FRP sheets. Fiber reinforced polymer (FRP) materials are composite materials consisting of high strength fibers immersed in a polymer matrix. The fibers in an FRP composite are the main load-carrying element and exhibit very high strength and stiffness when pulled in tension. An FRP laminate will typically consist of several million of these thin, thread-like fibers. The polymer matrix protects the fibers from damage, ensures that the fibers remain aligned, and allows loads to be distributed among many of the individual fibers in the composite. Shear strengthening of concrete beams using FRP is a topic that has been studied intensively, both theoretically and experimentally for more than a decade. Chen and Teng analyzed the shear failure of reinforced concrete (RC) beams strengthened with FRP and concluded that the distribution of stress in the FRP along the crack is non-uniform [8, 9, 10]. They presented a model for reinforced concrete beams

strengthened with FRP based on the fiber rupture and debonding. Aprile and Benedetti [11] presented a new flexural – shear design model for RC beams strengthened with EBR FRP systems. Ianniruberto and Imbimbo [12] derived a model based on the modified compression field theory combined with the variable angle truss model (that takes into account the influence of the FRP systems), in order to predict the contribution of FRP sheets to the shear capacity of RC beams. The shear bond model proposed by Zhang and Hsu [13] followed two approaches: model calibration by curve fitting and bond mechanism. The smallest reduction factor for the effective strain obtained from the two methods was suggested to be used. Aspects regarding lateral concrete peeling failure, under shear loading, of FRP were studied by Pellegrino and Modena [14]. This model follows the truss approach and describes the concrete, steel and FRP contribution to the shear capacity of RC beams based on the experimental observations made. Monti and Liotta [15] proposed a debonding model for the FRP-based shear strengthening of RC beams. This paper aims to investigate the effectiveness of using FRP sheets as an efficient strengthening method for reinforced concrete coupling beams. As a parametric study, three groups of RC coupling beams, of which two were strengthened by externally bonded FRP sheets and the other acted as a control model without strengthening have been analyzed and their responses are compared.

2. THEORETICAL ASPECTS

FRP systems have been shown to increase the shear strength of existing concrete beams and columns by wrapping or partially wrapping the members [16, 17, 18 and 19]. Orienting FRP fibers transverse to the axis of the member or perpendicular to potential shear cracks is effective in providing additional shear strength. Increasing the shear strength can also result in flexural failures, which are relatively more ductile in nature compared with shear failures [20].

Figure 2 shows three different types of FRP wrapping schemes used to increase the shear strength of rectangular beams, or columns. Completely wrapping the FRP system around the section on all four sides is the most efficient wrapping scheme and is most commonly used in column applications where access to all four sides of the column is usually available. In beam applications where an integral slab makes it impractical to completely wrap the member, the shear strength can be improved by wrapping the FRP system around three sides of the member (U-wrap) or bonding to two opposite sides of the member. Although all three techniques have been shown to improve the shear strength of a member, completely wrapping the section is the most efficient, followed by the three-sided U-wrap. Bonding to two sides of a beam is the least efficient scheme.

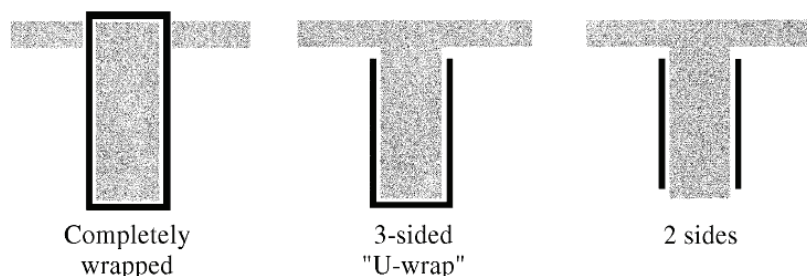


Fig. 2. Typical wrapping schemes for shear strengthening using FRP laminates [20]

The design shear strength of a concrete member strengthened with an FRP system should exceed the required shear strength. The required shear strength of an FRP-strengthened concrete member should be

computed with the load factors. The design shear strength should be calculated by multiplying the nominal shear strength by the strength reduction factor.

The nominal shear strength of an FRP-strengthened concrete member can be determined by adding the contribution of the FRP external shear reinforcement to the contributions from the reinforcing steel (stirrups, ties, or spirals) and the concrete. An additional reduction factor ψ_f is applied to the contribution of the FRP system.

$$\phi V_n \geq V_u \quad (1)$$

$$\phi V_n \geq \phi(V_c + V_s + \psi_f V_f) \quad (2)$$

In which:

V_n = nominal shear strength, N

ϕ = strength reduction factor

V_c = nominal shear strength provided by concrete with steel flexural reinforcement, N

V_f = nominal shear strength provided by FRP stirrups, N

V_n = nominal shear strength, N

V_s = nominal shear strength provided by steel stirrups, N

Figure 3 presents the variables used in shear-strengthening calculations for FRP laminates. The contribution of the FRP system to shear strength of a member is based on the fiber orientation and an assumed crack pattern [21]. The shear strength provided by the FRP reinforcement can be determined by calculating the force resulting from the tensile stress in the FRP across the assumed crack.

$$V_f = \frac{A_{fv} f_{fe} (\sin \alpha + \cos \alpha) d_f}{s_f} \quad (3)$$

$$A_{fv} = 2nt_f w_f \quad (4)$$

In which:

A_{fv} = area of FRP shear reinforcement with spacing s , mm²

f_{fe} = effective stress in the FRP; stress level attained at section failure, MPa

d_{fv} = effective depth of FRP shear reinforcement, mm

n = number of plies of FRP reinforcement

t_f = nominal thickness of one ply of FRP reinforcement, mm

w_f = width of FRP reinforcing plies, mm

The tensile stress in the FRP shear reinforcement at nominal strength is directly proportional to the level of strain that can be developed in the FRP shear reinforcement at nominal strength.

$$f_{fe} = \varepsilon_{fe} E_f \quad (5)$$

In which:

f_{fe} = effective stress in the FRP; stress level attained at section failure, MPa

ε_{fe} = effective strain level in FRP reinforcement attained at failure, mm/mm

E_f = tensile modulus of elasticity of FRP, MPa

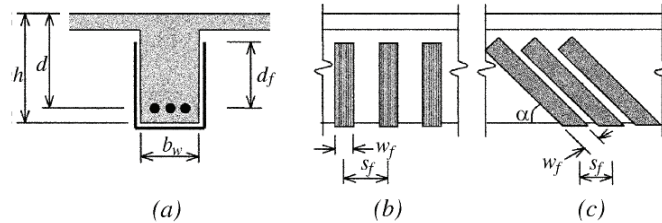


Fig. 3. Variables used in shear-strengthening calculations using FRP laminates [20]

3. VERIFICATION AGAINST EXPERIMENTAL DATA

a) General

In previous years some numerical studies on the shear behavior of RC members were performed applying the finite element method. Since its birth in the 1960s, the finite element method has become the most widely used numerical technique in structural analysis [22]. Although since that time there has been much research in this field, this method has not been generally consistent with design issues; the main reason for this is that although there is a great amount of experimental data available on the behavior of coupling beams, there has been little success in developing an applicable theoretical model to predict the behavior of coupling beam. In this study the decision was made to focus on generating a model that can predict the global behavior of coupling beams. Then, by analyzing the consequent results, the strengthening methods including the use of steel plates and FRP sheets are investigated. As the main purpose of this paper is investigation, the behavior of strengthened coupling beams by using finite element modeling, at least verifying the results of the control model against the available experimental data is unavoidable.

b) Experimental test

Coupled shear wall tested by Su and Zhu [23] was selected as a basis for verifying the numerical analysis. Figure 4 and 5 show the test setup and details of the specimen. In the test program, Loading was applied from a 500 kN actuator to the top end of each 90° rotated specimen through a rigid arm with the line of action passing through the beam center. So, the coupling beam was loaded with a constant shear force along the span and a linearly varying bending moment with the contra-flexure point at mid-span. In order to simulate the real situation in which the wall piers at the two ends of a coupling beam remain parallel under deflections of the building, a parallel mechanism was installed to connect the upper rigid arm with the lower structural steel beam fixed on the floor. Beam rotations (θ), defined as the differential displacement between the two beams ends in the loading direction divided by the clear span (l), were calculated using the displacements measured by linear variable displacement transducers (LVDTs).

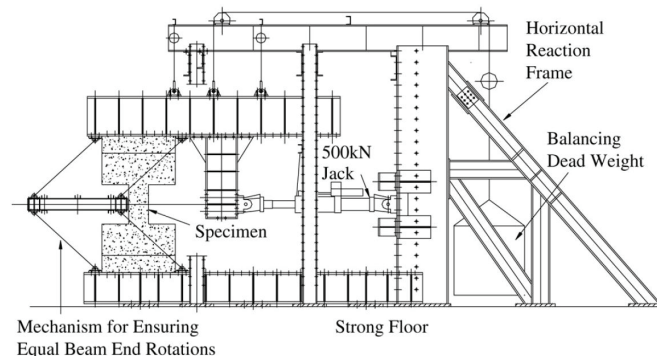


Fig. 4. Details of test setup [23]

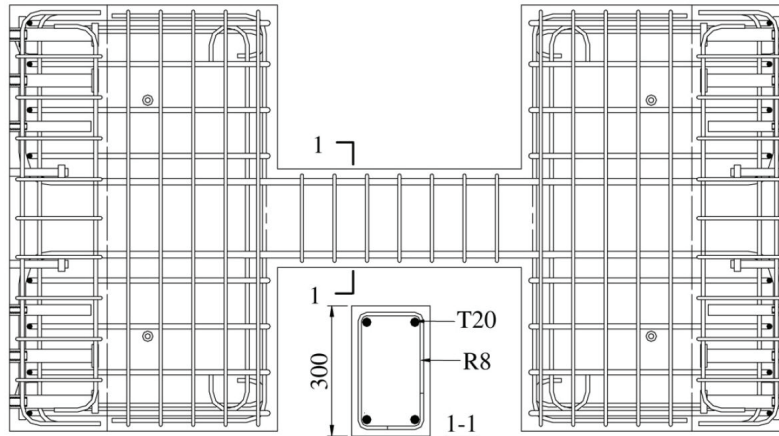


Fig. 5. Details of experimental specimen [23]

c) Modeling

The ANSYS finite element package was used to carry out the modeling and the solid65 element used to model the reinforced concrete. The solid65 element is a 3D isoparametric element, capable of cracking in tension and crushing in compression. This element is similar to the one proposed by Suidon and Schnobrich who introduced a 3D 20-node isoparametric element. The ANSYS element is defined by eight nodal points, each having three translational degrees of freedom x, y and z (and no rotation), along with a 2×2×2 Gaussian integration scheme which is used for the computation of the element stiffness matrix. The element has one solid material and up to three different reinforcing bars material properties can be defined. The most important feature of this element is that it can represent both the linear and nonlinear behavior of the concrete. For the linear stage, the concrete is assumed to be an isotropic material up to cracking. For the nonlinear part the concrete may experience plasticity and/or creep. The model is also capable of simulating the interaction between the two consequents, concrete and reinforcement. Thus, it can be used to describe the behavior of the reinforced concrete material.

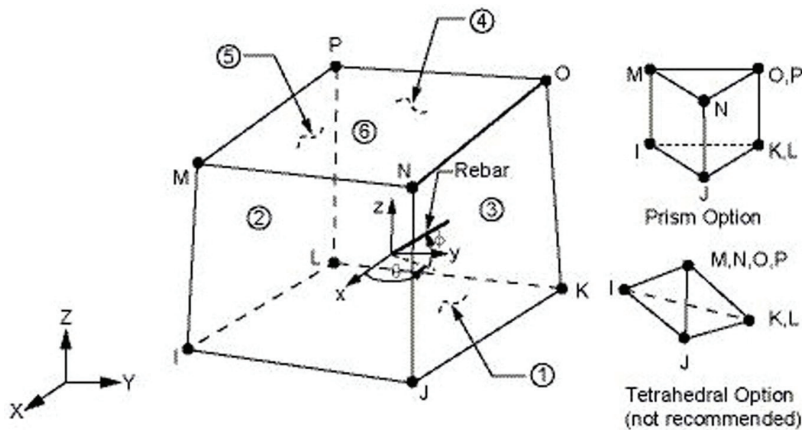


Fig. 6. Solid65 element [24]

The load is iterated step by step using the Newton-Raphson method. The outer face of the boundary element on the opposite side of the rigid arm is perfectly restrained against all degrees of freedom as shown in Fig. 7.

In the static analysis, the stress-strain relations of concrete are modified to represent the presence of a crack. A plane of weakness in a direction normal to the crack face and a shear transfer coefficient β_t (represents conditions of the crack face) are introduced in the Solid65 element. The shear strength

reduction for those subsequent loads, which induce shear across the crack surface, is considered by defining the value of β_t . This is important to accurately predict the loading after cracking, especially when calculating the strength of the concrete member dominated by shear, such as deep beams. The value β_t ranges from 0.0 to 1.0, with 0.0 representing a smooth crack (complete loss of shear transfer) and 1.0 representing a rough crack (no loss of shear transfer) [24]. The value of β_t used in many studies of reinforced concrete structures, however, varied between 0.05 and 0.25 [25, 26, 27]. A number of preliminary analyses were attempted in this study with various values for the shear transfer coefficient within this range, but convergence problems were encountered at low loads with β_t less than 0.2. Therefore, the shear transfer coefficient used in this study was equal to 0.2.

The density γ and the Poisson's ratio ν of concrete were assumed as 2400 kg/m^3 and 0.2. The shear transfer coefficient for a closed crack β_c was taken as 0.9. The ultimate uniaxial compressive strength f'_c introduced to the program was based on the experimental results [23].

Newton-Raphson equilibrium iterations were used for nonlinear analysis. A displacement controlled incremental loading was applied through a rigid arm. This was used to simulate the actual loading used in the experimental program. Automatic time stepping was used to control the load step sizes. Line search and the predictor-corrector methods were also used in the nonlinear analysis for accelerating the convergence. The failure of the coupling beam was defined when the solution for a small displacement increment did not converge. Consequently, the finite element model was constructed following the above-mentioned assumptions and considerations.

The control model (without strengthening) was designed according to seismic provisions to ensure that shear failure would occur prior to flexural failure.

In Fig. 7 the configuration of the model is shown with dimensions. Loading was applied to the top end of the 90 degree rotated model through a rigid arm element with the line of action passing through the beam centre as was also described in the experimental program. In this way, the coupling beam was loaded with a constant shear force along the span and a linearly varying bending moment with the extra-flexure point at mid-span.

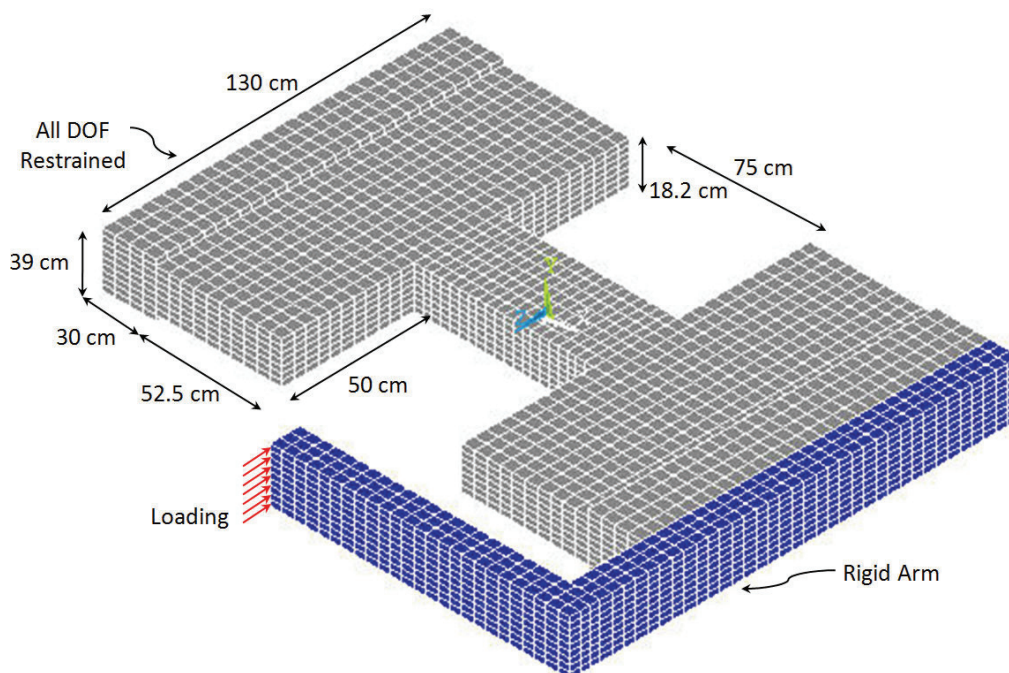


Fig. 7. Finite Element model (CM= Control Model)

The results of the analysis based on the above procedure are compared with the shear force-chord rotation angle of the experimental specimen and is shown in Fig. 8. On examination of the curves, it is obvious that the finite element model can predict the actual response measured by the experimental test with minimum inaccuracies. Also, it can be concluded that the numerical model is somehow stiffer than the experimental specimen, which is an evident consequence of finite element method. Considering the sufficient consistency of the numerical and experimental results for the coupling beam, the Control Model (CM) can be applied as a basic model for further parametric studies.

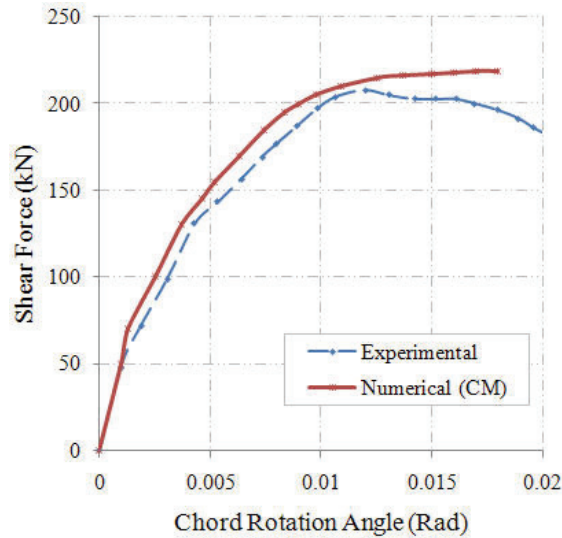


Fig. 8. Comparison of shear force-chord rotation curves for experimental and numerical models

4. PARAMETRIC STUDY

a) Steel plates

The strengthened models, by using steel plates, are generated and differ in plate thicknesses. The plates are modeled as attachments to the lateral faces of the coupling beams. The details of the coupling beams and material properties are presented in Tables 1 and 2 respectively.

Table 1. Details of coupling beams

Beam	Span-depth ratio	Plate thickness
CM	2.5	N/A
SP1	2.5	2.5 mm
SP2	2.5	5 mm

Table 2. Details of material properties for concrete and steel

Concrete	f_{cu} (MPa)	f'_c (MPa)
	50.2	43.9
Steel	f_y (MPa)	E (MPa)
	340	210000

Figure 9 shows the shear force-chord rotation behavior of the first strengthened coupling beam (named as SP1 with 2.5 mm steel plate) compared with the control model. The comparison of curves shows that the ultimate load has been upgraded from 219 kN to 312 kN which indicates an approximate 42% increase in the maximum load carried by the model. However, the chord rotation capacity has been improved slightly.

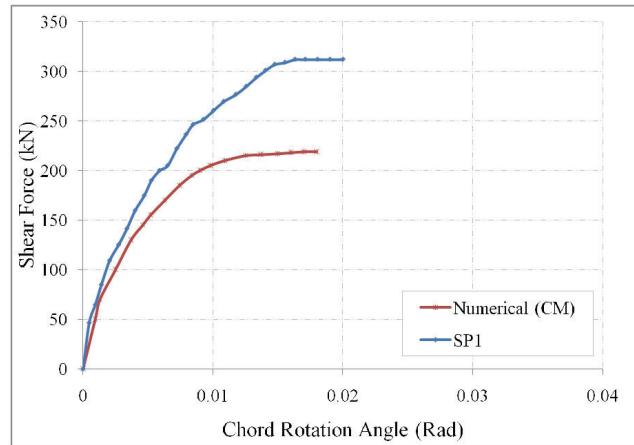


Fig. 9. Shear force-chord rotation curve for SP1 vs. control model

Figure 10 presents the shear force-chord rotation behavior of the second strengthened coupling beam (SP2) versus the control model. The increase in ultimate load is about 89%, which is considerable and indicates that using a steel plate with a proper thickness can significantly improve the behavior; in parallel with the latter result, the chord rotation capacity is increased by 25%.

Looking at the two curves shown in Fig. 11, one can see that there is a 33% increase in load capacity but a slight difference between chord rotations.

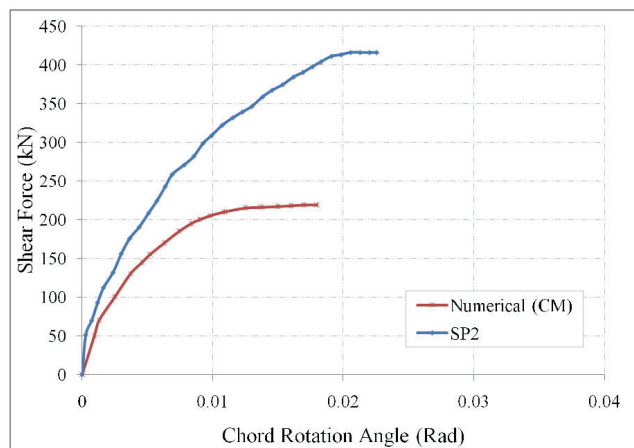


Fig. 10. Shear force-chord rotation curve for SP2 vs. control model

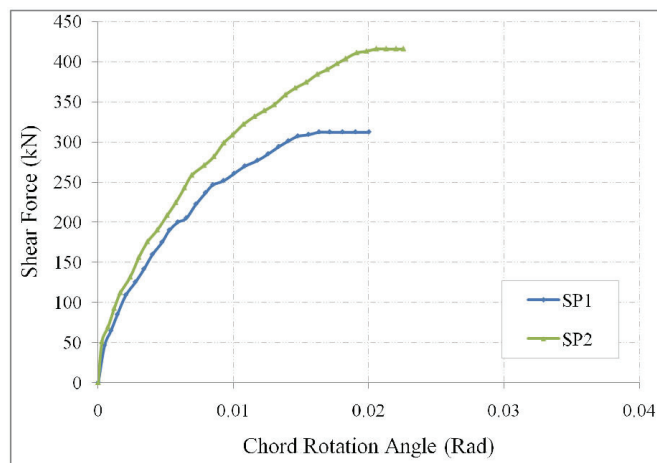


Fig. 11. Shear force-chord rotation curve for SP1 vs. SP2

b) Fiber reinforced polymers

A layered solid element, Solid46, was used to model the FRP composites. The geometry and node locations for this element type and the Schematic of FRP composites are shown in Fig. 12. The element allows for up to 250 different material layers with different orientations and orthotropic material properties in each layer. The element has three degrees of freedom at each node and translations in the nodal x, y, and z directions. To simulate the perfect bonding of the CFRP sheets with concrete, the nodes of Solid46 elements were connected to the nodes of Solid65 elements at the interface so that two materials shared the same nodes. The material properties for FRP composites are available from Table 1. It should be noted that modeling the contact of concrete and composite needs further specified research.

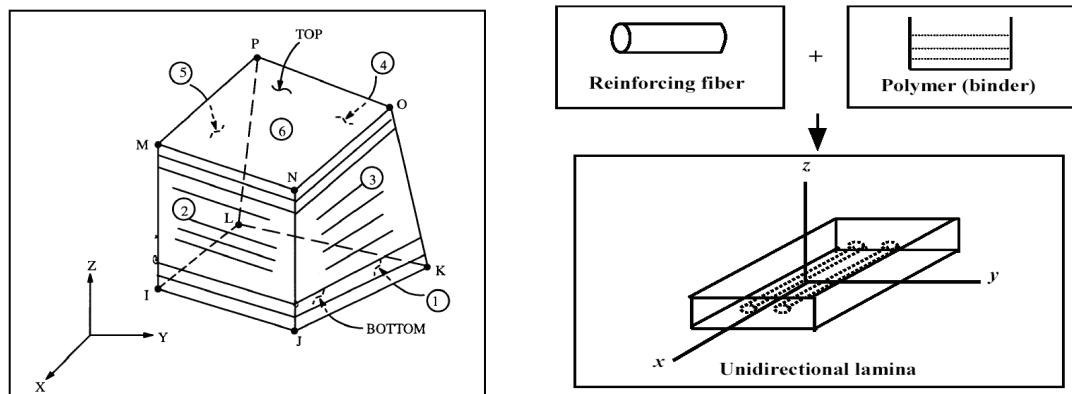


Fig. 12. Solid46 layered structural element and schematic of FRP composites (ANSYS 2004)

Parametric study was conducted to analyze two groups of RC coupling beams which were strengthened by externally bonded FRP sheets. Two FRP-strengthened groups differ on how the sheets are employed. In the first strengthened model the FRP sheets are attached to the faces of the beam (Fig. 13) and in the other, the coupling beam is strengthened by FRP-wrapping (Fig. 14). The thickness and properties of both groups are presented in Tables 3 and 4.

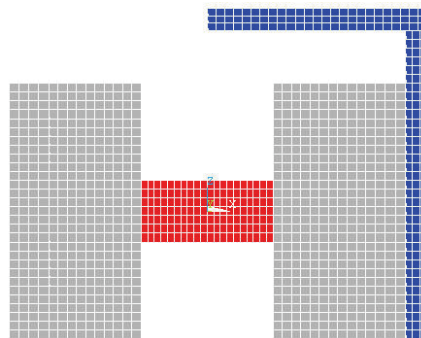


Fig. 13. Model with FRP sheets externally attached to the faces of coupling beam (FF)

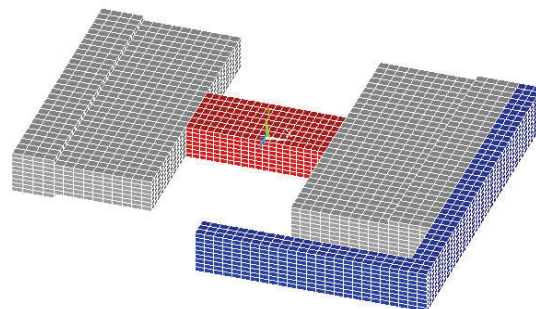


Fig. 14. Coupling beam strengthened with FRP wrap (FW)

Table 3. Details of different FRP-strengthened models

Model	Thickness (mm)	Properties
FF1	0.5	See Table 4
FF2	1.0	
FW1	0.5	
FW2	1.0	

Table 4. FRP material properties (ACI 440.2R-02)

FRP Composite	Elastic modulus (GPa)	Major poisson's ratio	Tensile strength (MPa)	Shear modulus (MPa)
CFRP	$E_x = 120$	$\nu_{xy} = 0.22$	1800	$G_{xy} = 4670$
	$E_y = 7$	$\nu_{xz} = 0.22$		$G_{xz} = 4670$
	$E_z = 7$	$\nu_{yz} = 0.30$		$G_{yz} = 770$

The results of FRP-strengthened model FF1 are compared with those of the control model and are shown in Fig. 15. As can be seen by the curves, the shear force-chord rotation behavior of the first FRP-strengthened coupling beam (FF1 with 0.5 mm thickness), the ultimate load has been upgraded from 219 kN to 292 kN which corresponds to the 33% increase in the maximum load carried by the model. The increase in the chord rotation capacity is also 33%. By considering the latest results, it can be found that improvement in both the load and rotation capacity is considerable.

Doubling the thickness of the FRP sheet (FF2) has increased the load capacity from 219 kN to 364 kN (that is equal to 66%) and chord rotation by 50 % compared with the control model as shown in Fig. 16.

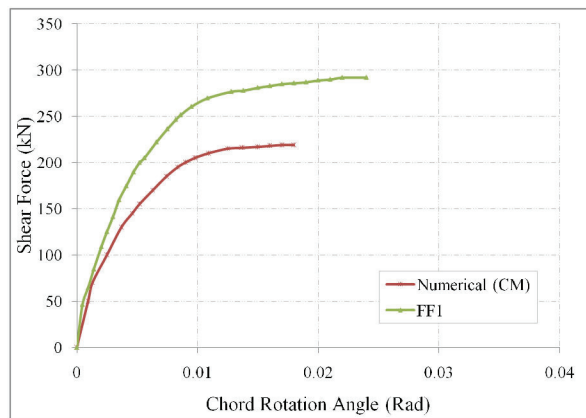


Fig. 15. Shear force-chord rotation curve for FF1 vs. control model

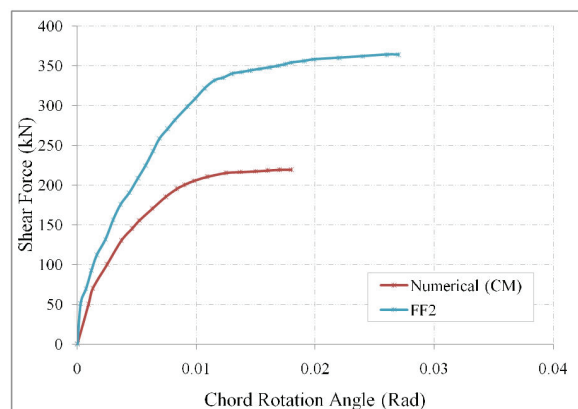


Fig. 16. Shear force-chord rotation curve for FF2 vs. control model

The results of FRP-strengthened model FW1 are compared with those of the control model and are shown in Fig. 17. As can be seen by the curves, the shear force-chord rotation behavior of the first FRP-wrapped coupling beam (FW1), the ultimate load has been upgraded from 219 kN to 314 kN which corresponds to a 43% increase in the maximum load carried by the model, approximately. The increase in the chord rotation capacity is 66%. By considering the latest results, it can be found that improvement rotation capacity is more considerable than for load capacity. Also, by concentrating on the curve, after reaching the point corresponding to about 300 kN, the ascending trend of the curve is mild in a wide range of chord rotation, indicating the more ductile behavior of the coupling beam.

Doubling the thickness of the FRP wrap (FW2) has increased the load capacity from 219 kN to 402 kN (that is equal to 84%) and chord rotation by 77 % compared with the control model as shown in Fig. 18. Compared with the control model, the increase in both the shear force and the chord rotation are quite close to each other.

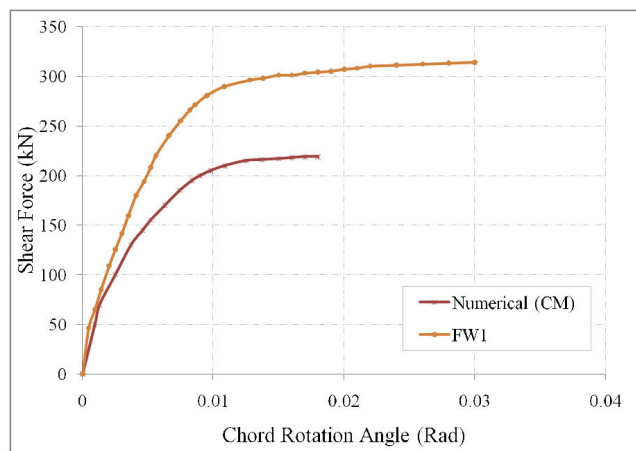


Fig. 17. Shear force-chord rotation curve for FW1 vs. control model

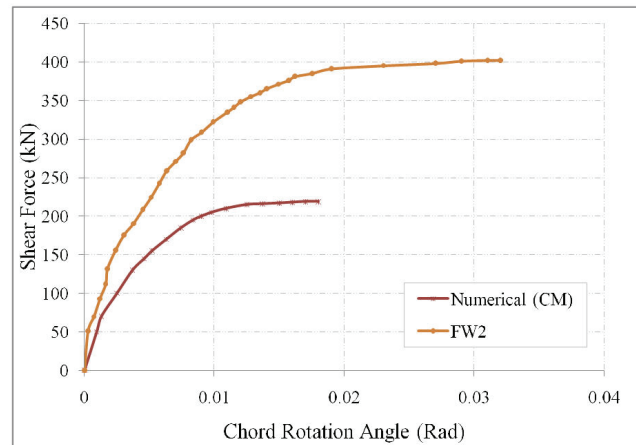


Fig. 18. Shear force-chord rotation curve for FW2 vs. control model

All of the curves for the FRP-strengthened models are compared with each other and shown in Fig. 19. The effect of thickness in strengthening changing from FF1 to FF2 has increased the ultimate load by 24%, while it upgraded the chord rotation capacity just 12%. On the other hand, this effect (increasing thickness by two times) in FRP-wrapped models (FW1 and FW2) has improved the load capacity up to 28%, but the increase in rotation is slight.

Comparing the results of FW2 and FF2, it can be found that the effect of FRP wrapping is better than using sheets on the faces of coupling beams, as the load capacity increase is about 11%, while the increase

in chord rotation angle is about 18%, leading to the observation that wrapping is the most effective technique for strengthening the coupling beams.

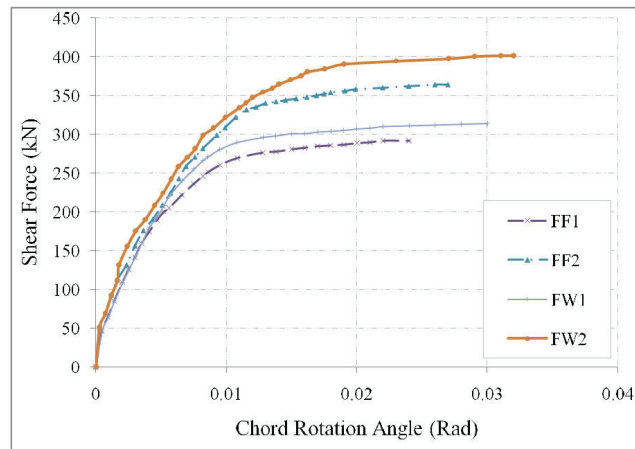


Fig. 19. Shear force-chord rotation curves for all FRP-strengthened models

As a distinct comparison between the results of models with externally bonded steel plates with those of the FRP-strengthened ones, Fig. 20 presents the curves of SP2 versus FW2. Considering the curves, it can be found that, although the steel plate increases the load capacity of the coupling beam up to 415 kN, which is 3% more than FW2, the chord rotation capacity of it is 41% less than that of FW2. This recent conclusion indicates that by using wrapped FRP around the coupling beam, the ductility behavior will be considerably improved.

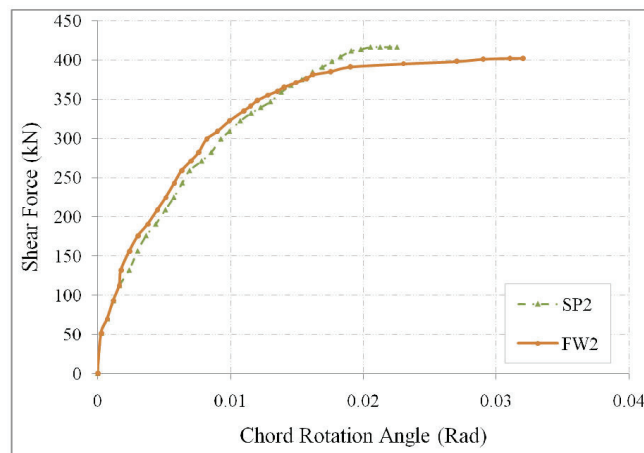


Fig. 20. Shear force-chord rotation curve for FW2 vs. SP2

5. CONCLUSION

From the discussion of the results obtained by analyzing different Finite Element models, the following conclusions can be drawn:

- Comparing the results of numerical analysis with the experimental test indicates that the finite element model can predict the actual response measured by the experimental test with minimum inaccuracies. Also, the numerical model is somehow stiffer than the experimental specimen as an evident consequence of finite element method.
- Shear force-chord rotation behavior of the first strengthened coupling beam (named as SP1 with 2.5 mm steel plates) compared with the control model showed that the ultimate load has been upgraded by 42%, but the chord rotation capacity has been improved only slightly.

- The behavior of the second strengthened coupling beam (SP2 with 5 mm plates) versus the control model indicated that the increase in ultimate load is about 89%, which is considerable. This can lead to the theory that using a steel plate with an optimized thickness can significantly improve the behavior; however, the deformation capacity is increased only 25%.
- Comparing the results of two plate-strengthened models, it can be seen that there is a 33% increase in the lateral load bearing capacity from SP1 to SP2 but a slight difference between chord rotations.
- The results of the first FRP-strengthened model in comparison with those of the control model indicate that shear force-chord rotation behavior of the first FRP-strengthened coupling beam (FF1 with 0.5 mm thickness) has been upgraded up to 33%. The increase in the chord rotation capacity is also 33%.
- Also, doubling the thickness of the FRP sheet (FF2) has increased the load capacity up to 66% and chord rotation by 50 % compared with control model.
- Shear force-chord rotation response of the first FRP-wrapped coupling beam (FW1) showed that the ultimate load has been upgraded up to 43%. The increase in the chord rotation capacity is 66%. So it can be found that improvement rotation capacity is more considerable than it is for load capacity. After reaching the point corresponding to about maximum load capacity, the ascending trend of the curve is mild in a wide range of chord rotation, which indicates the more ductile behavior of the coupling beam.
- Doubling the thickness of FRP wrap (FW2) has increased the load capacity up to 84% and chord rotation by 77 % compared with the control model.
- The effect of thickness in strengthening changing from FF1 to FF2 has increased the ultimate load by 24%, while upgrading the chord rotation capacity just 12%. On the other hand, this effect (increasing thickness by two times) in FRP-wrapped models (FW1 and FW2) has improved the load capacity up to 28% but the increase in rotation is slight.
- Comparing the results of FW2 and FF2, it can be found that the effect of FRP wrapping is better than using sheets on faces of coupling beams, as the load capacity increase is about 11%, while the increase in the chord rotation angle is about 18%, leading to the theory that wrapping is a more effective technique of strengthening the coupling beams.
- As a distinct comparison between the results of models with externally bonded steel plates with FRP-strengthened ones, it can be found that, although the steel plate increases the load capacity of the coupling beam up to 415 kN which is 3% more than FW2, its chord rotation capacity is 41% less than that of FW2. This recent conclusion indicates that by using wrapped FRP around the coupling beam, the ductility behavior will be considerably improved.

REFERENCES

1. Kheyroddin, A. & Naderpour, H. (2008). Nonlinear finite element analysis of composite RC shear walls. *Iranian Journal of Science & Technology, Transaction B: Engineering*, Vol. 32, No. B2, pp. 79-89.
2. El-Tawil, S. & Kuenzli, C. (2002). Pushover of hybrid coupled walls. II: Analysis and behavior. *Journal of the Structural Division*, ASCE, Vol. 128, No. 10, pp. 1282–9.
3. Harries, K. A., Moulton, J. D. & Clemson, R. L. (2004). Parametric study of coupled wall behavior—implications for the design of coupling beams. *Journal of Structural Engineering*, ASCE, Vol. 130, No. 3.
4. Park, W. & Yun, H. (2005). Seismic behavior of coupling beams in a hybrid coupled shear walls. *Journal of Constructional Steel Research*, Vol. 61, pp. 1492-1524.
5. Harries, K. A. (2001). Ductility and deformability of coupling beams in reinforced concrete shear walls. *Earthquake Spectra*, Vol. 17, No. 3, pp. 457–78.
6. Barnes, B. A., Baglin, P. S., Mays, G. C. & Subedi, N. K. (2001). External steel plate systems for the shear strengthening of reinforced concrete beams. *Journal of Engineering Structures*, Vol. 23, pp. 1162–76.

7. Subedi, N. K. & Baglin, P. S. (1998). External plate reinforcement for concrete beams. *Journal of Structural Engineering*, Vol. 124, No.12, pp. 1490–5.
8. Chen, J. F. & Teng, J. G. (2003). Shear capacity of fiber-reinforced polymer strengthened reinforced concrete beams: fiber reinforced polymer rupture. *Journal of Structural Engineering*, Vol. 129, No. 5, pp. 615-625.
9. Chen, J. F. & Teng, J. G. (2001). Anchorage strength models for FRP and steel plates bonded to concrete. *Journal of Structural Engineering*, Vol. 127, No. 7, pp. 784-791.
10. Chen, J. F. & Teng, J. G. (2003). Shear capacity of FRP-strengthened RC beams: FRP debonding. *Construction and Building Materials*, Vol. 17, pp. 27-41.
11. Aprile, A. & Benedetti, A. (2004). Coupled flexural-shear design of R/C beams strengthened with FRP. *Composites: Part B Engineering*, Vol. 35, pp. 1–25.
12. Ianniruberto, U. & Imbimbo, M. (2004). Role of fiber reinforced plastic sheets in shear response of reinforced concrete beams: Experimental and analytical results. *Journal of Composites for Construction*, Vol. 8, No. 5, pp. 415-424.
13. Zhang, Z. & Hsu, C. T. T. (2005). Shear strengthening of reinforced concrete beams using carbon-fiber-reinforced polymer laminates. *Journal of Composites for Construction*, Vol. 9, No. 2, pp. 158-169.
14. Pellegrino, C. & Modena, C. (2006). Fiber-reinforced polymer shear strengthening of reinforced concrete beams: Experimental study and analytical modeling. *ACI Structural Journal*, Vol. 103, No. 5, pp. 720-728.
15. Monti, G. & Liotta, M. A. (2007). Tests and design equations for FRP strengthening in shear. *Journal of Construction and Building Materials*, Vol. 21, pp. 799-809.
16. Malvar, L., Warren, G. & Inaba, C. (1995). Rehabilitation of navy pier beams with composite sheets. *Second FRP International Symposium on Non-Metallic (FRP) Reinforcement for Concrete Structures*, Ghent, Belgium, Aug., pp. 533-540.
17. Chajes, M., Januska, T., Mertz, D., Thomson, T. & Finch, W. (1995). Shear strengthening of reinforced concrete beams using externally applied composite fabrics. *ACI Structural Journal*, Vol. 92, No. 3, May-June, pp. 295-303.
18. Eshghi, S. & Zanjani-zadeh, V. (2008). Retrofit of slender square reinforced concrete columns with glass fiber-reinforced polymer for seismic resistance. *Iranian Journal of Science & Technology, Transaction B: Engineering*, Vol. 32, No. B5, pp. 437-450.
19. Mostofinejad, D. and Talaeitaba, S. B. (2006). Finite element modeling of RC connections strengthened with FRP laminates. *Iranian Journal of Science & Technology, Transaction B: Engineering*, Vol. 30, No. B1, pp. 21-30.
20. ACI 440.2R-08. (2008). Guide for the design and construction of externally bonded FRP systems for strengthening concrete structures. ACI Committee 440, American Concrete Institute.
21. Khalifa, A., Gold, W., Nanni, A. & Abel-Aziz, M. (1998). Contribution of externally bonded FRP to the shear capacity of RC flexural members. *Journal of Composites in Construction*, ASCE, Vol. 2, No. 4, pp. 195-203.
22. Kheyroddin, A., Hoseini Vaez, S. R. & Naderpour, H. (2008). Numerical analysis of slab-column connections strengthened with carbon fiber reinforced polymers. *Journal of Applied Sciences*, Vol. 8, No. 3, pp. 420-431.
23. Su, R. K. L. & Zhu, Y. (2005). Experimental and numerical studies of external steel plate strengthened reinforced concrete coupling beams. *Journal of Engineering Structures*, Vol. 27, pp. 1537-1550.
24. ANSYS, (2004). ANSYS User's Manual Revision 9.0, ANSYS, Inc., United States.
25. Bangash, M.Y.H. (1989). Concrete and concrete structures: Numerical modeling and applications. Elsevier Science Publishers Ltd., London, England.
26. Hemmaty, Y. (1998). Modeling of the shear force transferred between cracks in reinforced and fiber reinforced concrete structures. *Proceedings of the ANSYS Conference*, Pittsburgh, Pennsylvania. Vol. 1, pp. 123-138.
27. Huyse, L., Hemmaty, Y. & Vandewalle, L. (1994). Finite element modeling of fiber reinforced concrete beams. *Proceedings of the ANSYS Conference*, Pittsburgh, Pennsylvania. Vol. 2, pp. 72-84.